Adaptive Resolution Scheme for Non-additive Molecular Three-Body Potentials

Jose Alfonso Pinzon Escobar[1][0000−0003−0420−4230] and Philipp Neumann[2][0000−0001−8604−8846]

[1] Chair for High Performance Computing,
Helmut Schmidt University, Germany
jose.pinzon@hsu-hh.de
[2] High Performance Computing & Data Science, University of Hamburg, Germany
IT-Department, Deutsches Elektronen-Synchrotron, Germany
philipp.neumann@desy.de

Abstract. This work proposes the use of Adaptive Resolution Schemes (AdResS) in molecular dynamics simulations that include three-body interactions described by the Axilrod-Teller-Muto (ATM) potential. It is known that the computation of three-body forces greatly increases the number of calculations, which is the motivation to investigate appropriate speedup techniques. In this work, AdResS is used to allow for the computation of three-body interactions only within a portion of the simulation domain. This is implemented using force resolution regions, such that across the domain three-body forces are introduced smoothly from a pure two-body force region. The proposed scheme is tested using a relevant number of single-site, Lennard-Jones molecules in homogeneous case studies. In order to measure performance, the achieved speedup is expressed in terms of the geometric configuration of the force resolution regions where the three-body forces are calculated. These tests were carried out at node-level to measure the parallel and AdResS speedups using several force resolution region configurations with increasing portions of three-body presence. It is shown that AdResS, for three-body interactions, introduces inconsistencies in simple ensemble averages, like the temperature and density, which require the use of correction schemes. In this work we make use of the thermodynamic force for the correction of artificial density gradients in our simulations, which originate from a pressure difference induced by the coarse interactions.

Keywords: Molecular simulations · Adaptive resolution · Three-body interactions

1 Introduction

Molecular dynamics simulations are of increasing importance in the modeling of phenomena at the atomic level. The computation of interatomic forces requires a great portion of the computational effort within a simulation. Commonly, only short-range interactions are explicitly computed. Additionally, the calculated

ICCS Camera Ready Version 2026
To cite this paper please use the final published version:
DOI: 10.1007/978-3-032-29915-4_2

forces are limited to those within pairs of molecules. It is known that these limitations result in discrepancies between experimental and simulation results, e.g. for simple fluids. These differences can be corrected by introducing short-range, three-body interactions, such that the potential energy is given by

$$U = U\left(r_{ij}\right) + U\left(r_{ij}, r_{jk}, r_{ik}\right), \tag{1}$$

where r_{ij}, r_{jk}, r_{ik} are distances between particle pairs. Here, $U\left(r_{ij}\right)$ is described by the Lennard-Jones (LJ) potential [7], and $U\left(r_{ij}, r_{jk}, r_{ik}\right)$ is described by the ATM potential [3, 12]. The interactions are truncated at a distance r_c, the cutoff radius. The computation of $U\left(r_{ij}, r_{jk}, r_{ik}\right)$ dramatically increases the runtime and computational effort required by the simulation. Therefore, it is of interest to investigate techniques which allow for a faster calculation of these forces. In this work, the use of AdResS [15, 16] is proposed to speed up simulations that include the calculation of three-body interactions. Our technique builds on the fundamental AdResS literature for pairwise interactions, therefore combining two separate fields in a novel fashion. This could be used in the case of inhomogeneous scenarios, where the liquid phase is of main interest, or where the formation of vapor-liquid interfaces has to be studied instead of the behavior of the entire system.

This work is organized as follows. A theoretical overview of three-body interactions, AdResS, and molecular dynamics concepts used in our experiments is given in section 2, together with implementation details. In the following sections performance measurements are used to determine an appropriate force resolution region configuration for AdResS-enabled simulations. Subsequently, we present thermodynamic results generated using simulations of LJ fluids, as well as a discussion of the effects AdResS has on these thermodynamic properties. Using similar AdResS configurations, we show how the thermodynamic force could be used to correct unwanted effects on the ensemble averages. Finally, we give a conclusion and a perspective on future work.

2 Theoretical Background

2.1 Three-Body Forces in MD

The triple dipole described by the ATM potential contributes 5-10% of the total energy of a fluid in the liquid phase [5]. Additionally, it has been reported that introducing three-body computations can reduce the error of surface tension calculations with respect to experimental results from about 19% to 2.2%, see [4]. For this reason, the ATM potential has been introduced to inhomogeneous simulations of the vapor-liquid phases of LJ fluids [17] and argon [18]. These facts highlight the importance of using three-body forces in molecular dynamics simulations.

The ATM potential is given by

$$U_{ijk} = \nu \left(\frac{1 + \cos\theta_i \cos\theta_j \cos\theta_k}{\left(r_{ij} r_{jk} r_{ik}\right)^3} \right), \tag{2}$$

ICCS Camera Ready Version 2026
To cite this paper please use the final published version:
DOI: 10.1007/978-3-032-29915-4_2

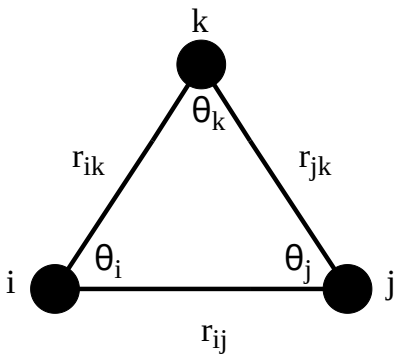

Fig. 1: Triangular configuration formed by three atoms i, k, j. The interactions are truncated if any of the distances r_{ij}, r_{jk}, r_{ik} are larger than r_c.

where ν is a molecular model-dependent constant. The angles $\theta_i, \theta_j, \theta_k$ and lengths r_{ij}, r_{jk}, r_{ik} are associated with the triangular configuration formed by an atomic triplet, as shown in fig. 1.

The dependence on the angles can be removed using the law of cosines, which also allows for the implementation of Newton's third law [10] to significantly reduce the required force calculations. For instance, a reduction factor of 9 can be achieved in some cases [14]. In this work, the interactions are truncated if any of the three sides of the triangular configuration are larger than a cutoff radius r_c, as for instance in [2, 13].

2.2 Adaptive Resolution

AdResS is used with the purpose of reducing the computational effort required by the calculation of the forces in molecular dynamics. This is achieved by reducing the level of resolution of the molecules. Originally, it has been applied to reducing the degrees of freedom (DoFs) by coarsening a multi-site molecule to a single site located at the center of mass [15]. The coarse interactions are computed using a corresponding coarse potential, for instance following the procedure given in [11].

Here, certain aspects of AdResS are used to introduce three-body interactions to a region of the domain, without requiring DoF reduction nor the use of coarse-grain potentials as the one proposed in [9]. The used approach is illustrated in fig. 2. Three force resolution regions are used to transition from pure, two-body interactions, $\boldsymbol{F} = \boldsymbol{F_{ij}}$, to a two- and three-body scheme, $\boldsymbol{F} = \boldsymbol{F_{ij}} + \boldsymbol{F_{ijk}}$. The former corresponds to the coarse force (CF) region, and the latter to the full force (FF). These are connected by a hybrid force (HF) region, where $\boldsymbol{F} = \boldsymbol{F_{ij}} + w\left(x\right)\boldsymbol{F_{ijk}}$ via a weight function $w\left(x\right)$, as in regular AdResS.

ICCS Camera Ready Version 2026
To cite this paper please use the final published version:
DOI: 10.1007/978-3-032-29915-4_2

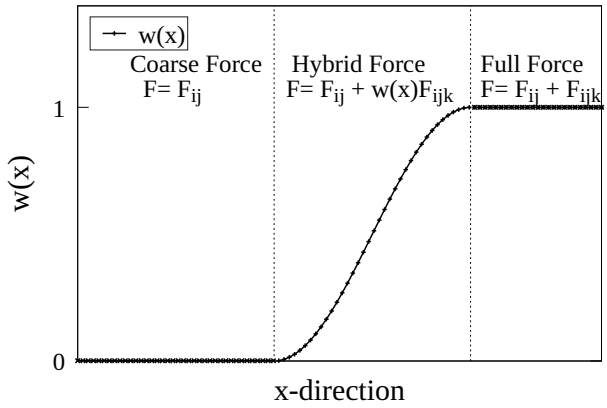

Fig. 2: The CF and FF regions are connected via an HF region. A weight function, $w(x)$, smoothly introduces $\boldsymbol{F_{ijk}}$ to the domain. The x-direction can be any of the principal physical directions of a 3D domain.

In the HF region, the transition from CF to FF is enabled via $w(x)$,the weight function given by

$$w(x) = \begin{cases} 0 & x \in \text{ CF} \\ \cos^2\left[\left(\frac{\pi}{2\,d_{HF}}\right)(x - d_{FF})\right] & x \in \text{ HF} \\ 1 & x \in \text{ FF}, \end{cases} \tag{3}$$

as in [20], and where d_{HF} and d_{FF} are the widths of the HF and FF regions respectively, and x is the position of a given molecule. It allows for a smooth introduction of the three-body forces into the simulation.

Using this proposed scheme, it is attempted to reproduce fluid properties in a slab of the domain with two- and three-body interactions. These properties should match those of a reference simulation, where three-body interactions were used across the complete domain. In the AdResS simulation, the FF slab has to be sufficiently wide to allow for meaningful physical results, as well as for a significant reduction of the computational effort.

2.3 Algorithmic Implementation

The three-body computations, as described in section 2.1, are combined with the AdResS aspects of section 2.2 to speed up the computation of three-body interactions. It is assumed that the atomic triplets can be found efficiently, for instance through the use of the linked cells algorithm and appropriate cell traversing routines, as in [14].

The implementation is described in algorithm 1. In the context of this work, the molecules are sorted into cells. At least one of the involved cells must be fully

ICCS Camera Ready Version 2026
To cite this paper please use the final published version:
DOI: 10.1007/978-3-032-29915-4_2

or partially inside the HF or FF regions. A molecular triplet can be sorted into a single, a pair, or a triplet of cells. Based on the spatial distribution sketched in fig. 2, determining to which resolution region a molecular triplet belongs to, is a fundamental task. For this reason, before traversing the molecules, the cells are used to determine if the computation of three-body forces is required. If this is the case, then algorithm 1 is used to compute the required interactions.

Our approach is limited to flat interfaces, splitting the domain over a unique dimension x. In traditional AdResS, as given e.g. in [15], the center of mass for a multi-site molecule is used for the computation of $w(x)$. In our case, this approach is discouraged, because the center of mass would need to be computed for every triplet. This would greatly increase the overhead, which would drastically reduce the achieved performance. Therefore, we make use of the average position over x, i.e. $\bar{x}$, of a given atomic triplet. This is given by

$$\bar{x} = \frac{1}{3}(x_1 + x_2 + x_3) \tag{4}$$

where x_1, x_2, x_3 are the x-direction components of the positions of each of the three molecules. In this way, the value of the weight function can be determined as $w(\bar{x})$. However, the choice of (4) above COM was made for performance reasons only. In our tested scenarios using equal mass, single-site molecules, the two methods are equivalent and yield the same results.

Algorithm 1 Computation of ATM Forces using AdResS

Require: At least on cell partially/fully in HF or FF
1: **for all** molecular triplets in cells **do**
2: Find $\bar{x}$ with (4)
3: Determine which resolution region
4: Calculate $w(\bar{x})$ with (3)
5: Compute $\boldsymbol{F} = \boldsymbol{F_{ij}} + w(\bar{x})\,\boldsymbol{F_{ijk}}$
6: **end for**

2.4 Measured Property

Here, we describe the measured thermodynamic properties for the validation of the proposed AdResS and three-body methodology. Our main focus is to measure the particle distribution, as well as thermal and mechanical equilibrium. The density and temperature can be directly measured over the x-dimension of the domain via binning on every time step. Their average over the time steps can then be presented. In this way, a profile for both functions, $\langle \rho(x) \rangle$ and $\langle T(x) \rangle$, can be generated. Further details can be found in [1].

Mechanical equilibrium can be described by the pressure. As mentioned in section 2.1, this property is greatly affected by the presence of three-body interactions, as compared to the results obtained only with two-body forces, e.g. in

ICCS Camera Ready Version 2026
To cite this paper please use the final published version:
DOI: 10.1007/978-3-032-29915-4_2

[2], where pure LJ results are compared to those including the ATM potential. Thus, measuring the pressure can allow for a better understanding of the effects of AdResS on the simulation domain. In order to generate a pressure profile, the pressure tensor, $\bar{\mathbf{P}}$, has to be measured over x. Here, the Irving-Kirkwood representation is used

$$\bar{\mathbf{P}}(x) = \rho(x)\,\kappa_B T\mathbf{1} + \frac{1}{2A}\left\langle \sum_{i=1}^{N-1}\sum_{j>i}^{N} \boldsymbol{r}_{ij} \otimes \boldsymbol{F}_{\boldsymbol{ij}} \frac{1}{|x_{ij}|}\theta\left(\frac{x - x_i}{x_{ij}}\right)\theta\left(\frac{x_j - x}{x_{ij}}\right)\right\rangle, \tag{5}$$

where θ is a Heaviside function, x indicates the discrete bin centers positions, x_i and x_j the positions of particles i and j over the x-dimension, A is the bin surface area perpendicular to x, and $\otimes$ stands for the outer product between two vectors. The first term on the r.h.s. of (5) stands for the ideal gas part of P, in analogy to the global pressure value commonly used in molecular dynamics. The second r.h.s. term is referred to as the virial or excess contribution. In equilibrium, the off-diagonal terms of $\bar{\mathbf{P}}$ are zero. Then the remaining diagonal terms can be split into two different components called the normal and tangential parts [1, 19],

$$p_N(x) = P_{zz} \tag{6}$$

$$p_T(x) = \frac{1}{2}(P_{xx} + P_{yy}) \tag{7}$$

where P_{xx}, P_{yy}, P_{zz} are the three diagonal terms of $\bar{\mathbf{P}}$. In equilibrated, homogeneous regions the equality $p_N = p_T$ is fulfilled and $p_N =$ constant over x.

In this context, we make use of $\bar{\mathbf{P}}$ to measure the local effects of AdResS on the pressure in the FF and HF regions. The main focus is on measuring and reproducing $p_N(x)$ with different values widths of the FF and HF slabs, and comparing the obtained results to those of a reference simulation with ATM forces everywhere. Together with $\rho(x)$ and $T(x)$, these ensemble averages illustrate the effects of AdResS over fundamental ensemble averages.

3 Results

Here we present results for simulations involving single-site LJ fluids. As mentioned before, the pairwise forces are given by the LJ potential, while the ATM potential describes the three-body interactions. This section starts by using homogeneous scenarios for the measurement of the speedup in the context of the configuration of the force resolution regions, i.e. the width of the regions where $\boldsymbol{F}_{\boldsymbol{ijk}}$ is computed. These studies are useful for finding a proper width to the FF and HF regions, while allowing for meaningful performance gains. This is followed by the presentation of thermodynamic averages and correlation functions as given in section 2.4, comparing simulations with three-body computations across the whole domain to those with the optimal configurations found with the speedup studies.

Throughout this section, we make use of LJ-reduced units for all given quantities. This reduction scheme can be found in [1]. The used molecular model is

ICCS Camera Ready Version 2026
To cite this paper please use the final published version:
DOI: 10.1007/978-3-032-29915-4_2

set to LJ parameters of $\epsilon = 1$ and $\sigma = 1$, and a mass $m = 1$. For all cases, the ATM parameter is set to $\nu = 0.072$ as in [2]. The simulations were carried out using our in-house molecular dynamics simulation software, `LauraMD` [14]. It is programmed in C++ and parallelized using OpenMP.

3.1 Speedup

AdResS is used to reduce the computational effort of computing the forces in a simulation. In [8], this was measured in terms of the speedup gained in terms of the region configuration.

Similarly, here we use the fraction v, given by

$$v = \frac{V_{HF} + V_{FF}}{V_{Total}}, \tag{8}$$

to indicate the portion of the total domain's volume V_{Total}, where the three-body forces have to be computed, i.e, the sum of the FF and HF volumes, V_{FF} and V_{HY} respectively. The limit cases are $v = 1$, where $\boldsymbol{F_{ijk}}$ is computed over all the domain and $v = 0$, where no three-body forces are present at all. Given that only slab geometries are used in this work, v can be also expressed in terms of the widths of the HF and FF, respectively d_{HF} and d_{FF}.

With this in mind, the achieved AdResS-speedup for a given configuration can be measured via

$$S_{AdResS} = \frac{t_{3B}}{t_{3BAdResS}}, \tag{9}$$

where the runtimes correspond to the computation of the three-body forces, and t_{3B} is the limit case for $v = 1.0$, while $t_{3BAdResS}$ is the corresponding runtime for a scenario with a known v-value.

In this context, v determines the total computational effort. Opposed to the methodology given in [8], for this case there is no reduction of the degrees of freedom (the number of sites), therefore we cannot directly use the speedup relation given therein. However, we can use a similar procedure by measuring several v-values to determine the value that allows for a large total FF + HF volume while retaining a large speedup. In theory, it would be expected for S_{AdResS} and t to be linear functions of v. However, the AdResS functionalities add overhead, which hampers down the performance.

The AdResS and parallel speedups were measured for a box domain with $a = 40$. A total of $N = 20,000$ molecules were used, and the linked cells algorithm was used with $r_c = 2.5$ and a total of $4,096$ cells with periodic boundary conditions on all domain borders. The phase space was first equilibrated for $50,000$ time steps and $\Delta t = 0.01$, to guarantee an even distribution of the molecules across the domain. This was followed by a production phase of 20 time steps to measure the runtime, t, of the routine which computes the three-body forces.

The parallel performance results are given in fig. 3 for increasing proportions of v. For all cases V_{FF} was maintained at 10% of V_{Total}, with the remaining v-portion being assigned to V_{HF}. All configurations were run 5 times, and the

ICCS Camera Ready Version 2026
To cite this paper please use the final published version:
DOI: 10.1007/978-3-032-29915-4_2

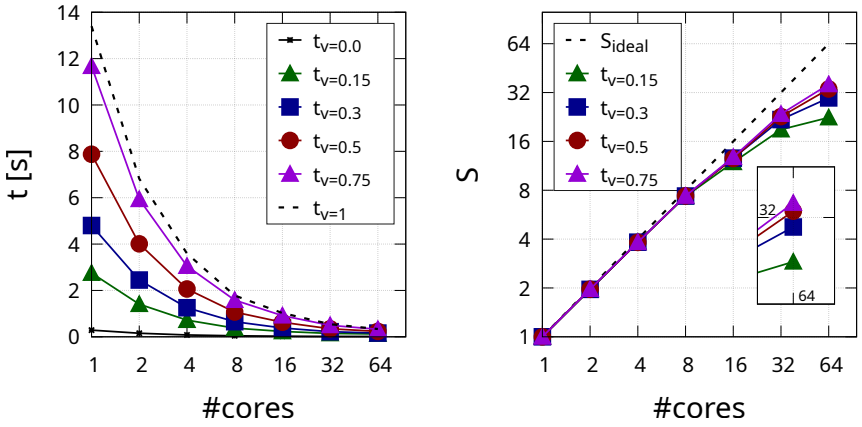

Fig. 3: Strong scaling and parallel speedup for a domain with side length $a = 40$ and $N = 20,000$ molecules, measured over 20 steps. Several v-values are tested. A lower value of v means that the ATM potential is computed in a smaller portion of the domain. For $v = 0.0$, the given runtime shows the overhead introduced by the AdResS functionalities. On the right-hand side, a magnification of the highest core count is given within the figure.

average of these runs is presented. Their respective standard deviations are negligible. The runtimes for the limiting cases, $v = 0.0$ and $v = 1.0$, are given for comparison.

As expected, decreasing values of v allow for a faster production run. However, the overhead seems to accumulate as v increases. This is more noticeable at low core counts, where it is seen that for $v = 0.75$ the runtime does not decrease linearly with v. A similar case is found for $v = 0.5$, which is above the 50% expected time reduction. From fig. 3, we learn that $v = 0.3$ allows for a scenario with good speedup, while being close to the theoretical runtime reduction.

As the core count increases, these differences become less apparent, since also the reference time is decreased. Therefore, it is important to measure the performance in terms of the AdResS speedup for varying number of cores. This is given in fig. 4. The runtime of a simulation with $v = 1.0$ was used as t_{3B} at different core counts, and used in (9) as the full three-body reference simulation. The tested values are then $v = \{0.15, 0.3, 0.5, 0.75, 1.0\}$. A higher v together with the overhead results in a reduced performance, for instance at $v = 0.5$. However, for all core counts the scenario $v = 0.3$ allows for a production run twice as fast as t_{3B}. These results can help decide what proportion of three-body computation domain should be used to guarantee a significant performance increase. In this context, we see a small v, could allow for noticeable performance gains while retaining sufficient FF domain to generate meaningful results.

ICCS Camera Ready Version 2026
To cite this paper please use the final published version:
DOI: 10.1007/978-3-032-29915-4_2

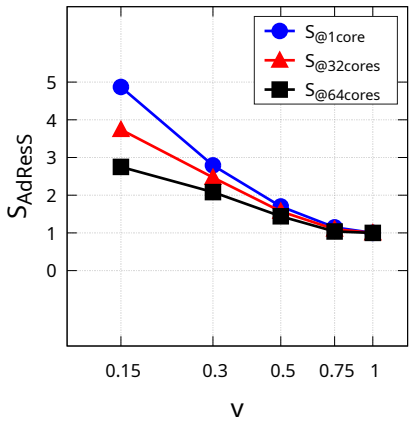

Fig. 4: AdResS-Speedup for several core counts and v-values. Higher values of v reduce the achieved performance gain, as seen e.g. for $v = 0.5$. For each core count, the corresponding t_{3B} was used with $v = 1.0$, as given in (9).

3.2 Thermodynamical Results

This section presents results which measure the properties described in section 2.4, e.g. the pressure tensor components. The AdResS-enabled simulations were configured following the insight obtained from section 3.1, such that the force resolution regions can be optimally configured. In this sense, the FF and HF regions were set using $v \in \{0.3, 0.5, 1.0\}$ and $v = 1.0$ is used as a reference. As before, for the other configurations of v, FF is set to 10% of V_{Total} while only the proportion of HF varies.

These simulation runs were configured as before. The time step was set to $\Delta t = 0.003$ with $T = 1.2$. After every step, a velocity scaling thermostat was used to adjust the temperature. The given properties were sampled over $50,000$ time steps, using a total of 500 bins. As mentioned in section 2, it is known that the ATM potential can have large effects on the pressure of the system [4]. Therefore, the given results are based on measuring $p_N(x)$ over the simulation domain, since for a homogeneous region it is expected that $p_N = \text{constant}$.

These results are given in fig. 5, for the aforementioned v-values. The FF region is constant for all cases and indicated by the two solid lines, while HF varies with v. The borders for each v-value are indicated by the differently dashed lines. Profiles for $T(x)$, $\rho(x)$, and $p_N(x)$ are provided as time averages. The results for $v = 1.0$ are used as a pure three-body reference.

It is seen that AdResS introduces artificial density gradients towards the FF region. While the density values in CF appear closer to the original bulk density ρ_0, the gradients generate visible deviations as the three-body forces are introduced. A similar case is observed in $T(x)$, where a slight deviation with respect to the reference is observed. Nevertheless, this appears to be below 5%

ICCS Camera Ready Version 2026
To cite this paper please use the final published version:
DOI: 10.1007/978-3-032-29915-4_2

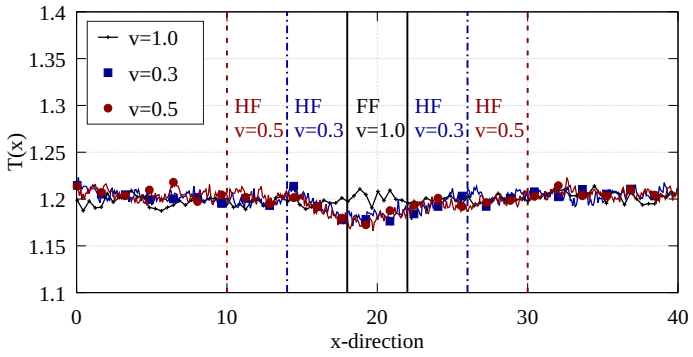

(a) Temperature, $T\,(x)$

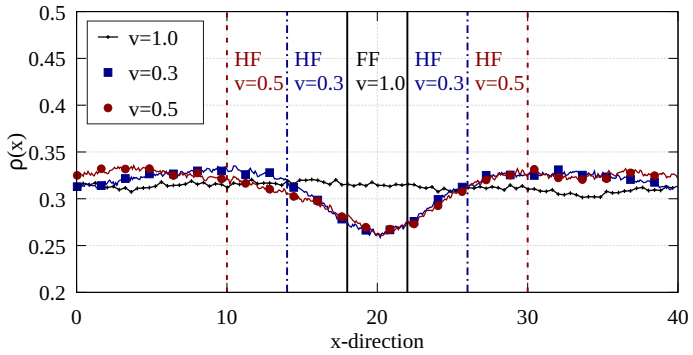

(b) Density, $\rho\,(x)$

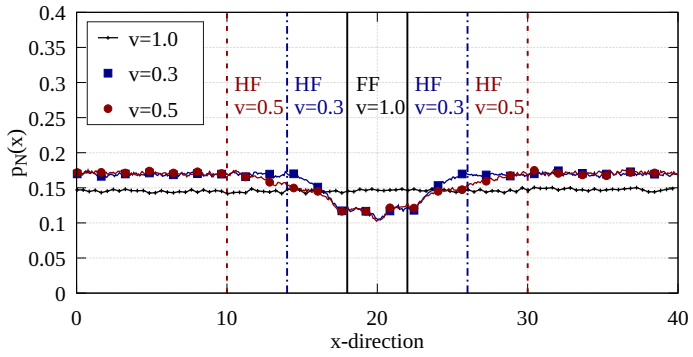

(c) Normal pressure tensor component, $p_N\,(x)$

Fig. 5: (a) Temperature profile, (b) density profile, and (c) normal pressure component, $p_N\,(x)$, of $\bar{\mathbf{P}}$, for $v \in \{1.0, 0.5, 0.3\}$. The force resolution region borders are correspondingly labeled by v value, as well as using solid lines for FF and dashed lines for HF. The values of $v = 1.0$ correspond to the pure three-body reference. These profiles were sampled using 500 bins for $50,000$ time steps. The use of AdResS generates computational artifacts in the sampled profiles with respect to the reference $v = 1.0$.

ICCS Camera Ready Version 2026
To cite this paper please use the final published version:
DOI: 10.1007/978-3-032-29915-4_2

of the bulk temperature $T = 1.2$ and is assumed to have negligible effects on the other measured properties. However, major AdResS effects can be observed in the $p_N(x)$ profile. Both tested scenarios deviate greatly from the reference p_N value, particularly at the FF region. Noticeably, the bulk value at the CF region also deviates from that of $v = 1.0$. Since the density, $\rho(x)$, contributes to the ideal part of $\bar{\mathbf{P}}$ as given in (5), a density correcting scheme was used as a possible correction to the p_N deviations observed in fig. 5.

3.3 Thermodynamic Force

Algorithm 2 Thermodynamic Force Computation

Require: *sampling*, *stride*, *step*, α, ρ_0
  for all *step* in simulation **do**
    ⋮
    Sample $\rho(x)$
    if $(step > sampling)$ & $(step \mod stride = 0)$ **then**
      Compute $\boldsymbol{F}^i_{Th.}$ using (10)
    end if
    Apply $\boldsymbol{F}^i_{Th.}$ to all molecules
    ⋮
  end for

The encountered issues in fig. 5 are very similar to those found in the implementation of traditional, DoF-reducing AdResS. For instance, artificial density gradients have been reported in AdResS implementations [15]. As mentioned before, the direct relation between $\bar{\mathbf{P}}$ and $\rho(x)$ could be used to investigate correction schemes of benefit to both properties.

A standard approach, e.g. [6], to fixing these issues makes use of an iterative method to compute a correction of the density via its gradient, such that

$$\mathbf{F}^{i+1}_{Th.}(x) = \mathbf{F}^i_{Th.}(x) - \frac{\alpha}{\rho_0^2}\left(\nabla \rho^i(x)\right), \tag{10}$$

where α is a given constant, and ρ_0 is the bulk density, which is known a priori.

The thermodynamic force is computed using the methodology described in [20, 6]. Our implementation is given in algorithm 2. The $F_{th.}$ update is done on every *stride* steps. At the beginning of the simulation, a *sampling* number of steps is allowed before the first update, $\boldsymbol{F}^0_{Th.}$, so that a smooth density profile is obtained. Once the *sampling* threshold is surpassed, $\boldsymbol{F}^i_{Th.}$ is updated every *stride* number of steps using (10). Since $\rho(x)$ is sampled using bins, the same approach is used for $\boldsymbol{F}_{Th.}(x)$. For this, central differences are used to compute $\nabla\rho(x)$. Once the updated iterate $\boldsymbol{F}^i_{Th.}(x)$ is stored in every bin, its value is linearly interpolated and applied to every molecule. The computation of $\boldsymbol{F}_{Th.}$

ICCS Camera Ready Version 2026
To cite this paper please use the final published version:
DOI: 10.1007/978-3-032-29915-4_2

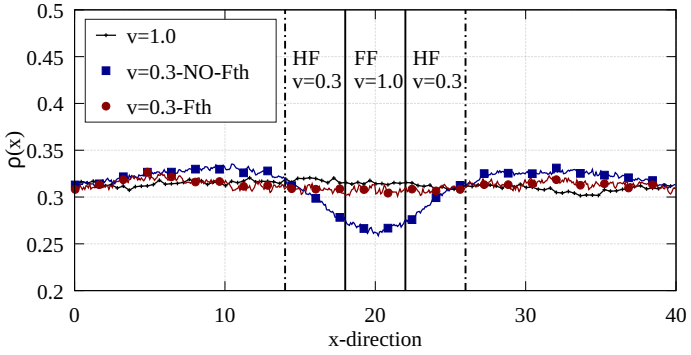

(a) Corrected density profile, $\rho\,(x)$

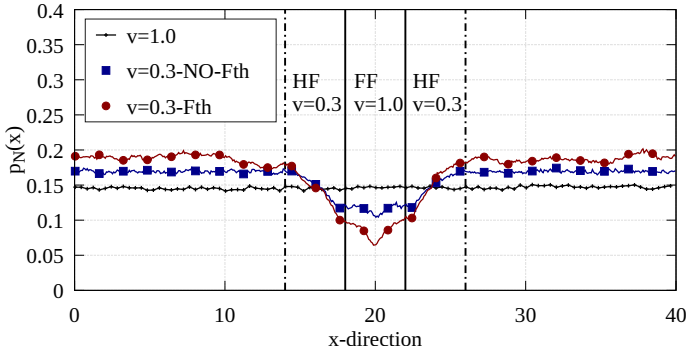

(b) The normal pressure tensor component profile, $p_N\,(x)$

Fig. 6: (a) Correction to the density profile and (b) effects on the normal component. Although $\boldsymbol{F}_{Th.}$ corrected the density over x, the sampled values of p_N show that the thermodynamic force had negative effects on this property. The FF region is indicated by solid black lines, and the HF region by dashed lines.

ICCS Camera Ready Version 2026
To cite this paper please use the final published version:
DOI: 10.1007/978-3-032-29915-4_2

can be finalized either with a convergence criterion or after a total number of steps.

Tests were performed using the $v = 0.3$ configuration. A first *sampling* run of $20,000$ steps was used to generate a smooth density profile, and *stride* was set to 100 steps. This was followed by an $F_{th.}$ calculation and property sampling production run of $50,000$ steps, during which the thermodynamic force was updated following algorithm 2. The value of $\alpha = 0.01$ was heuristically determined with test runs.

The results are given in fig. 6 for the density and normal pressure tensor component profiles, $\rho(x)$ and $p_N(x)$ respectively. As expected, $\boldsymbol{F}_{Th.}$ successfully corrected the deviations of $\rho(x)$ observed in fig. 5. The resulting profile closely follows the reference value of $v = 1.0$. However, the obtained values of $p_N(x)$ seem to be negatively affected by $\boldsymbol{F}_{Th.}$. It can be seen that the value in the CF region also seems to be affected by the use of the thermodynamic force. The reasons for this are a matter of ongoing investigation.

4 Conclusion and Outlook

In this work an AdResS approach for the computation of three-body interactions was presented, since these computations greatly increase the workload and impact the runtime. It was shown that it is possible to reduce the workload by restricting the calculation of three-body forces to only a portion of the domain via the use of AdResS.

Simple LJ fluids were used to test the described AdResS and three-body implementation. Moreover, the presented results show that in some cases it is possible to speed up the simulation fivefold when compared to a reference case with three-body forces present everywhere. The performance gains were presented in terms of a fraction v, which quantifies the portion of the domain where three-body interactions are computed. Although in theory the AdResS speedup is a linear function of v, this is different in the multicore case, where the overall computational load saturates earlier for smaller values of v. We have investigated and quantified these speedups for the provided scenarios. Therefore, parallel studies were carried out to determine appropriate values of v for which there are sufficient performance gains while still allowing for the generation of meaningful physical results.

We proposed several correlation functions and ensemble averages for the validation of the proposed methodology. These showed that AdResS introduced non-physical artifacts to the two- and three-body regions. Specifically, the density profile was visibly affected by the use of AdResS, which introduced unwanted density gradients around the interface borders. These are commonly reported in the AdResS literature and are corrected using a thermodynamic force scheme. The latter was introduced in this work via an iterative approach. With it the density profile was corrected, but the measured pressure tensor components were not successfully reproduced.

ICCS Camera Ready Version 2026
To cite this paper please use the final published version:
DOI: 10.1007/978-3-032-29915-4_2

Nevertheless, it was shown that there is great speedup to be achieved by the use of AdResS in the context of three-body forces. Additionally, further work will be done on determining how to introduce the thermodynamic force to the computation of the pressure tensor, this could help correct the negative effects on the normal pressure tensor component. And on how the thermodynamic force affects the temperature of the AdResS with three-body simulations. Our studies were limited to single phase molecular systems, however three-body forces are of great interest in multi-phase simulations. Thus, ongoing work will target the possible use of AdResS in the vapor-liquid phase interaction for which appropriate correcting schemes might need to be developed.

Acknowledgments. Support, including resources by hpc.bw, funded by dtec.bw – Digitalization and Technology Research Center of the Bundeswehr, is acknowledged. dtec.bw is funded by the European Union – NextGenerationEU. The project has been supported by the BMBF project 3xa, 16ME0653, which has been financed by the European Union.

Disclosure of Interests. The authors have no competing interests to declare.

References

[1] Michael P. Allen and Dominic J. Tildesley. *Computer Simulation of Liquids*. Oxford University Press, June 2017. ISBN: 9780198803195. DOI: 10.1093/oso/9780198803195.001.0001.

[2] Phil Attard. "Simulation results for a fluid with the Axilrod-Teller triple dipole potential". In: *Phys. Rev. A* 45 (8 Apr. 1992), pp. 5649–5653. DOI: 10.1103/PhysRevA.45.5649.

[3] B. M. Axilrod and E. Teller. "Interaction of the van der Waals Type Between Three Atoms". In: *The Journal of Chemical Physics* 11.6 (June 1943), pp. 299–300. ISSN: 0021-9606. DOI: 10.1063/1.1723844.

[4] J.A. Barker. "Surface tension and atomic interactions in simple liquids". In: *Molecular Physics* 80.4 (1993), pp. 815–820. DOI: 10.1080/00268979-300102671.

[5] J.A. Barker, R.A. Fisher, and R.O. Watts and. "Liquid argon: Monte Carlo and molecular dynamics calculations". In: *Molecular Physics* 21.4 (1971), pp. 657–673. DOI: 10.1080/00268977100101821.

[6] S. Fritsch et al. "Adaptive resolution molecular dynamics simulation through coupling to an internal particle reservoir". In: *Phys. Rev. Lett.* 108 (17 Apr. 2012), p. 170602. DOI: 10.1103/PhysRevLett.108.170602.

[7] John A. Zollweg J. Karl Johnson and Keith E. Gubbins. "The Lennard-Jones equation of state revisited". In: *Molecular Physics* 78.3 (1993), pp. 591–618. DOI: 10.1080/00268979300100411.

[8] Christoph Junghans, Animesh Agarwal, and Luigi Delle Site. "Computational efficiency and Amdahl's law for the adaptive resolution simulation technique". In: *Computer Physics Communications* 215 (2017), pp. 20–25. ISSN: 0010-4655. DOI: https://doi.org/10.1016/j.cpc.2017.01.030.

ICCS Camera Ready Version 2026
To cite this paper please use the final published version:
DOI: 10.1007/978-3-032-29915-4_2

[9] Luca Larini, Lanyuan Lu, and Gregory A. Voth. "The multiscale coarse-graining method. VI. Implementation of three-body coarse-grained potentials". In: *The Journal of Chemical Physics* 132.16 (Apr. 2010), p. 164107. ISSN: 0021-9606. DOI: 10.1063/1.3394863.

[10] Gianluca Marcelli. *The role of three-body interactions on the equilibrium and non-equilibrium properties of fluids from molecular simulation*. Jan. 2001. DOI: 10.25916/sut.26273536.v1.

[11] Timothy C. Moore, Christopher R. Iacovella, and Clare McCabe. "Derivation of coarse-grained potentials via multistate iterative Boltzmann inversion". In: *The Journal of Chemical Physics* 140.22 (June 2014), p. 224104. DOI: 10.1063/1.4880555.

[12] Y. Muto. "Force between nonpolar molecules". In: *Proc. Phys.-Math. Soc. Jpn.* 17.6 (1943), pp. 629–631. ISSN: 0370-1239.

[13] Isabel Nitzke, Sergey V. Lishchuk, and Jadran Vrabec. "Long-Range Corrections for Molecular Simulations with Three-Body Interactions". In: *Journal of Chemical Theory and Computation* 21.1 (2025). PMID: 39686577, pp. 1–4. DOI: 10.1021/acs.jctc.4c01250.

[14] José Alfonso Pinzón Escobar et al. "Linked cell traversal algorithms for three-Body interactions in molecular dynamics". In: *Computer Physics Communications* 321 (2026), p. 110028. ISSN: 0010-4655. DOI: https://doi.org/10.1016/j.cpc.2026.110028.

[15] Matej Praprotnik, Luigi Delle Site, and Kurt Kremer. "Adaptive resolution molecular-dynamics simulation: Changing the degrees of freedom on the fly". In: *The Journal of Chemical Physics* 123.22 (Dec. 2005), p. 224106. ISSN: 0021-9606. DOI: 10.1063/1.2132286.

[16] Matej Praprotnik et al. "Adaptive resolution simulation of liquid water". In: *Journal of Physics: Condensed Matter* 19.29 (July 2007), p. 292201. DOI: 10.1088/0953-8984/19/29/292201.

[17] Richard J. Sadus. "Exact calculation of the effect of three-body Axilrod–Teller interactions on vapour–liquid phase coexistence". In: *Fluid Phase Equilibria* 144.1 (1998), pp. 351–359. ISSN: 0378-3812. DOI: https://doi.org/10.1016/S0378-3812(97)00279-3.

[18] Richard J. Sadus and J. M. Prausnitz. "Three-body interactions in fluids from molecular simulation: Vapor–liquid phase coexistence of argon". In: *The Journal of Chemical Physics* 104.12 (Mar. 1996), pp. 4784–4787. ISSN: 0021-9606. DOI: 10.1063/1.471172.

[19] J.P.R.B. Walton et al. "The pressure tensor at the planar surface of a liquid". In: *Molecular Physics* 48.6 (1983), pp. 1357–1368. DOI: 10.1080/00268978300100971.

[20] Han Wang, Christof Schütte, and Luigi Delle Site. "Adaptive Resolution Simulation (AdResS): A Smooth Thermodynamic and Structural Transition from Atomistic to Coarse Grained Resolution and Vice Versa in a Grand Canonical Fashion". In: *Journal of Chemical Theory and Computation* 8.8 (2012). PMID: 26592127, pp. 2878–2887. DOI: 10.1021/ct3003354.

ICCS Camera Ready Version 2026
To cite this paper please use the final published version:
DOI: 10.1007/978-3-032-29915-4_2